

Accurate Redetermination of the X-ray Structure and Electronic Bonding in Adenosylcobalamin

Lizhi Ouyang, Paul Rulis, and W. Y. Ching*

Department of Physics, University of Missouri—Kansas City, Kansas City, Missouri 64110

Giorgio Nardin and Lucio Randaccio*

Centre of Excellence in Biocrystallography—Department of Chemical Sciences, University of Trieste, 34127 Trieste, Italy

Received July 18, 2003

The electronic structure of adenosylcobalamin (B_{12} coenzyme, AdoCbl) has been calculated by a density functional method, using the orthogonalized linear combination of the atomic orbital method (OLCAO). Since a fixed accurately determined geometry was needed in such calculations, the crystal structure of adenosylcobalamin has been redone and refined to $R = 0.065$, using synchrotron diffraction data. Comparison with the recently reported electronic structures of cyano- (CNCbl) and methylcobalamin (MeCbl) shows that the net charges and bond orders vary only on the axial donors. The values in the three cobalamins suggest that the Co–C bond in MeCbl has a strength similar to that in AdoCbl, but it is significantly weaker than that in CNCbl. Present results are compared with those previously reported for the analogous corrin derivatives; i.e., simplified cobalamins with the side chains **a–f** replaced by H atoms. Despite a qualitative agreement, a discrepancy in the calculated HOMO–LUMO gap is found.

Introduction

The B_{12} cofactors so far known are alkylcobalamins (RCbl) consisting of a cobalt corrinoid with a pendant nucleotide (with different purine base), which occupies five of the six coordination sites of an octahedral Co(III). The sixth position is occupied by the R group or by a CN ligand in the cyanocobalamin (CNCbl), the vitamin B_{12} itself (Scheme 1). CNCbl is not a biologically active species, whereas the cobalamins having R = methyl (methylcobalamin, MeCbl) and 5'-deoxy-5'-adenosyl (coenzyme B_{12} , AdoCbl) are cofactors of several enzymes. All the currently known reactions of B_{12} -dependent enzymes involve the making and breaking of the Co–C bond.¹

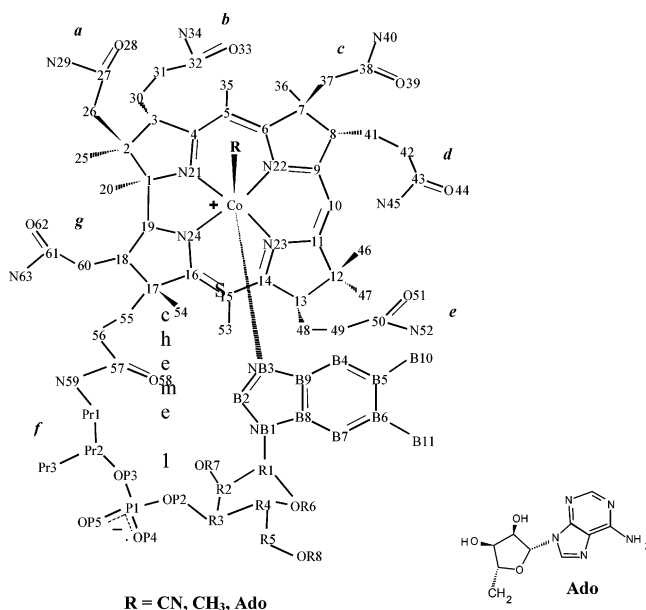
The MeCbl-based enzymes (methyltransferases) catalyze the transfer of methyl groups, and the overall mechanistic scheme requires a reversible *heterolytic* cleavage of the Co–Me bond.²

The process catalyzed by AdoCbl-based enzymes (isomerase and eliminase) proceeds through a stepwise process initiated

* To whom correspondence should be addressed. E-mail: randaccio@univ.trieste.it (L.R.).

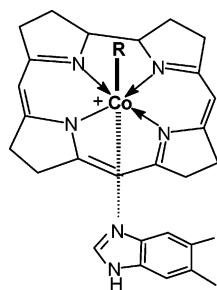
- (1) *Vitamin B₁₂ and B₁₂ Proteins*; Kräutler, B. D., Arigoni, B. D., Golding, B. T., Eds.; Wiley-VCH: Weinheim, 1998. *Chemistry and Biochemistry of B₁₂*; Banerjee, R., Ed.; J. Wiley & Sons: New York, 1999.
- (2) Matthews, R. G. *Acc. Chem. Res.* **2001**, *34*, 681–689.

Scheme 1



by the *hemolytic cleavage* of the Co–C bond.³ The homolysis rate in the enzyme is increased by a factor of about 10^{12} , with respect to the free coenzyme. How such a spectacular

Scheme 2



acceleration is achieved by the interaction with the apoenzyme is a subject of debate and is not adequately understood at present.³ The first structural determinations of B₁₂ enzymes (isomerase and methyltransferase)⁴ indicated that the benzimidazole moiety (Scheme 1) moves away from cobalt (base-off form) and is replaced by a histidine residue of the protein. Thus, this was thought to be related in some way to the homolysis acceleration. However, the X-ray structure of an eliminase has recently shown that no benzimidazole displacement occurs in this enzyme.⁵

It is clear that the understanding of the factors influencing the Co–C bond cleavage also requires an in-depth study of the electronic structure and bonding in cobalamins. Detailed knowledge of the electronic properties of the Co–C bond should also be instrumental in answering some additional basic questions, such as which factors determine the different behavior of MeCbl and AdoCbl toward the Co–C cleavage? Accurate theoretical calculations on the isolated coenzymes should, in principle, reveal the specific electronic features that discriminate the Co–Me and Co–Ado bonds. Furthermore, the physicochemical properties, such as spectroscopic data, of such biomolecules appear somewhat conflicting^{6–9} and could find an explanation on firm theoretical grounds.

Theoretical calculations were attempted in the past on simple models¹⁰ and on the positively charged RCo–corrin (Scheme 2), which are simplified cobalamins with the side chains a–f (Scheme 1) replaced by the H atoms. These studies^{11,13} were based on semiempirical approaches and

sometimes reached conflicting conclusions. Only recently has the density functional theory (DFT) been applied to alkyl-corrin complexes, with a dramatic increase in the number of papers.^{14,15} However, accurate geometric parameters of the molecule are very important for the linear combination of the atomic orbital (LCAO) method. Until a few years ago, structural data on cobalamins were of low accuracy, preventing meaningful comparison. The structure of the B₁₂ coenzyme has been extensively studied by means of X-ray¹⁶ and neutron diffraction.¹⁷ However, these studies did not attain an accuracy dramatically better than those obtained by Lenhart in the early structural determination.¹⁸ Therefore, Kratky and Kräutler stated¹⁹ that it is highly desirable that an X-ray high-resolution structure of the coenzyme B₁₂ become available. Analogously, a low-resolution structure of MeCbl was reported many years ago.²⁰ Only recently, thanks to the use of the synchrotron X-ray source coupled with area detectors (for high-speed data collection) as well as improvement in the crystallization techniques, has accurate structural data of several cobalamins been obtained,²¹ including the redetermination of CNCbl and MeCbl.²²

On the basis of these accurate structural data, we have recently calculated the electronic structure of CNCbl²³ and MeCbl²⁴ by a first-principles method using for the first time the complete cobalamin molecule including the side chains (Scheme 1). These calculations have been found fully consistent with UV–vis, XES, and XPS experimental data. Now, we extend this theoretical approach to the complete molecule of AdoCbl. Since our DFT approach requires fixed

- (3) Marzilli, L. G. In *Bioinorganic Catalysis*; Reedijk, J., Bouwman, E., Eds.; Marcel Dekker: New York, 1999; pp 423–468.
- (4) Drennan, C.; Huang, S.; Matthews, R. G.; Ludwig, M. L. *Science* **1994**, *266*, 1669–1674. Mancina, F.; Keep, N. J.; Nakagawa, A.; Leadly, P. F.; McSweeney, S.; Rasmussen, B.; Bosecke, P.; Diat, P.; Evans, P. R. *Structure* **1996**, *4*, 339–350.
- (5) Shibata, N.; Masuda, J.; Tobimatsu, T.; Toraya, T.; Suto, K.; Morimoto, Y.; Yasuoka, N. *Structure* **1999**, *7*, 997–1008.
- (6) Dong, S.; Padmakumar, R.; Banerjee, R.; Spiro, T. G. *J. Am. Chem. Soc.* **1996**, *118*, 9182–9183. Dong, S.; Padmakumar, R.; Maiti, N.; Banerjee, R.; Spiro, T. G. *J. Am. Chem. Soc.* **1998**, *120*, 9947–9948. Dong, S.; Padmakumar, R.; Banerjee, R.; Spiro, T. G. *J. Am. Chem. Soc.* **1999**, *121*, 7063–7070.
- (7) Puckett, J. M., Jr.; Mitchell, M. B.; Hirota, S.; Marzilli, L. G. *Inorg. Chem.* **1996**, *25*, 4656–4662.
- (8) Hay, B. P.; Finke, R. G. *J. Am. Chem. Soc.* **1987**, *109*, 8012–8018.
- (9) Kumar, M.; Qiu, D.; Spiro, T. G.; Ragsdale, S. W. *Science* **1995**, *270*, 628–630.
- (10) Christianson, D. W.; Lipscomb, W. N. *J. Am. Chem. Soc.* **1985**, *107*, 2682–2686. Hansen, L. M.; Pavan Kumar, P. N. V.; Marynick, D. S. *Inorg. Chem.* **1994**, *33*, 728–735. Mealli, C.; Sabat, M.; Marzilli, L. G. *J. Am. Chem. Soc.* **1987**, *109*, 1593–1594.
- (11) Zhu, L.; Kostic, N. M. *Inorg. Chem.* **1987**, *26*, 4194–4197.
- (12) Hansen, L. M.; Derecskei-Kovacs, A.; Marynick, D. S. *J. Mol. Struct.* **1998**, *431*, 53–57.
- (13) Rovira, C.; Kunc, K.; Hutter, J.; Parrinello, M. *Inorg. Chem.* **2001**, *40*, 11–17.
- (14) (a) Andruniow, T.; Zgierski, M. Z.; Kozłowski, P. M. *J. Phys. Chem. B* **2000**, *104*, 10921–10927. (b) Randaccio, L.; Geremia, S.; Nardin, G.; Stener, M.; Toffoli, D.; Zangrando, E. *Eur. J. Inorg. Chem.* **2002**, 93–103. (c) Jensen, K. P.; Saur, S. P. A.; Liljefors, T.; Norrby, P. O. *Organometallics* **2001**, *20*, 550–556. (d) Jensen, K. P.; Ryde, U. *J. Phys. Chem. A* **2003**, *107*, 7539–7545. (e) Dölker, N.; Maseras, F.; Lledos, A. J. *J. Phys. Chem. B* **2003**, *107*, 306–315. (f) Andruniow, T.; Zgierski, M. Z.; Kozłowski, P. M. *J. Chem. Phys.* **2002**, *115*, 7522–7533. (g) Jensen, K. P.; Ryde, U. *J. Mol. Struct. (THEOCHEM)* **2002**, *585*, 239–255.
- (15) (a) Andruniow, T.; Zgierski, M. Z.; Kozłowski, P. M. *J. Am. Chem. Soc.* **2001**, *123*, 2679–2680. (b) Andruniow, T.; Zgierski, M. Z.; Kozłowski, P. M. *J. Phys. Chem. A* **2002**, *106*, 1365–1373.
- (16) Savage, H. F. J.; Finney, J. L. *Nature* **1986**, *322*, 717–720. Savage, H. F. J.; Lindley, P. F.; Finney, J. L.; Timmins, P. A. *Acta Crystallogr., Sect. B* **1987**, *B43*, 280–295.
- (17) Bouquiere, J. P.; Finney, J. L.; Savage, H. F. J. *Acta Crystallogr., Sect. B* **1994**, *B50*, 566–578. Bouquiere, J. P.; Finney, J. L.; Lehmann, M. S.; Lindley, P. F.; Savage, H. F. J. *Acta Crystallogr., Sect. B* **1993**, *B49*, 79.
- (18) Lenhart, P. G. *Proc. R. Soc. London, Ser. A* **1968**, *A303*, 45–84.
- (19) Kratky, C.; Kräutler, B. In *Chemistry and Biochemistry of B₁₂*; Banerjee, R., Ed.; J. Wiley & Sons: New York, 1999; pp 9–41.
- (20) Rossi, M.; Glusker, J. P.; Randaccio, L.; Summers, M. F.; Toscano, P. J.; Marzilli, L. G. *J. Am. Chem. Soc.* **1985**, *107*, 1729–1738.
- (21) Kratky, C.; Färber, G.; Gruber, K.; Deuter, Z.; Nolting, H. F.; Konrat, R.; Kräutler, B. *J. Am. Chem. Soc.* **1995**, *117*, 4654–4670. Brown, K. L.; Cheng, S.; Zubkowski, J. D.; Valente, E. J.; Kropton, L.; Marques, H. M. *Inorg. Chem.* **1997**, *36*, 3666–3675. Randaccio, L.; Furlan, M.; Geremia, S.; Slouf, M. *Inorg. Chem.* **1998**, *37*, 5390–5393. Randaccio, L.; Geremia, S.; Nardin, G.; Slouf, M.; Srnova, I. *Inorg. Chem.* **1999**, *38*, 4087–4092.
- (22) Randaccio, L.; Furlan, M.; Geremia, S.; Slouf, M.; Srnova, I. *Inorg. Chem.* **2000**, *39*, 3403–3413.
- (23) Ouyang, L.; Randaccio, L.; Rulis, P.; Kurmaev, E. Z.; Moewes, A.; Ching, W. Y. *J. Mol. Struct.* **2003**, *622*, 221–227.
- (24) Kurmaev, E. Z.; Moewes, A.; Ouyang, L.; Randaccio, L.; Rulis, P.; Ching, W. Y. *Europhys. Lett.* **2003**, *62*, 582–587.

Table 1. Crystal Data and Structure Refinement for AdoCbl

formula	C ₇₂ H ₁₀₀ CoN ₁₈ O ₁₇ P·1.25(C ₂ H ₆ O)·8.25(H ₂ O)
fw	1800.83
T, K	100(2)
λ, Å	0.737
cryst syst; struct group	orthorhombic; P2 ₁ 2 ₁ 2 ₁
a, Å	15.194(15)
b, Å	21.32(2)
c, Å	27.55(3)
V, Å ³	8923(16)
Z; ρ _{calcd} , Mg/m ³	4; 1.341
μ, mm ⁻¹	0.295
F(000)	3834
crystal size, mm	0.20 × 0.20 × 0.50
refinement method	full-matrix least squares on F ²
data/restraints/params	19149/0/1113
goodness-of-fit on F ²	1.001
final R indices [I > 2σ(I)]	R1 ^a = 0.066, wR2 ^b = 0.187
R indices (all data)	R1 = 0.067, wR2 = 0.188

$${}^a R1 = \sum ||F_o| - |F_c|| / \sum |F_o|. \quad {}^b wR2 = [\sum w(|F_o|^2 - |F_c|^2)^2 / \sum w|F_o|^2]^{1/2}.$$

highly accurate structural data, the X-ray analysis of AdoCbl based on synchrotron data is also reported.

Experimental Section

Crystallization. Commercial samples of AdoCbl, with a stated purity by the manufacturer of about 98%, were from Fluka. Several attempts to grow single crystals by the hanging drop method under different conditions²² led to red parallelepiped-shaped crystals, some of which were used to collect diffraction data. However, the subsequent data analysis showed that these crystals were of low quality. By contrast, successive attempts to grow single crystals by slow evaporation of AdoCbl water solution after the addition of acetone were successful, and one of these crystals was used for the final data collection.

X-ray Data Collection and Crystal Structure Refinement. Data collection was carried out at the X-ray diffraction beamline of the Elettra synchrotron (Trieste, Italy) using the rotating crystal method and a 345 mm Mar image plate. Crystals were mounted in a loop and frozen to 100 K, using a nitrogen stream cryocooler. Intensity data were processed using the program DENZO and scaled and merged using the program SCALEPACK.^{25a} Friedel pairs were not merged (anomalous dispersion included), and no absorption correction was applied. The structure was solved starting from the previously determined coordinates and refined by the full-matrix least-squares method using SHELXL-97.^{25b} Crystal data and structure refinement details are displayed in Table 1.

Theoretical Method. The electronic structure of AdoCbl, using the newly determined structure, was calculated by the ab initio orthogonalized linear combination of the atomic orbital method (OLCAO)²⁶ based on the density functional theory (DFT)²⁷ in its local density approximation (LDA).²⁸ Similar calculations for CNCbl and MeCbl have been reported.^{23,24} The OLCAO method is an all-electron method particularly suitable for large complex crystals and molecules. In the OLCAO method, the basis functions are expanded in terms of atomic orbitals, which are themselves

formed as linear combinations of Gaussian-type orbitals (GTO). The LDA potential is constructed from the total charge density and is conveniently written as a sum of atom-centered functions, which also consist of GTOs. This facilitates the evaluation of various types of multicenter integrals with no limitations on their ranges of interaction. There are several special advantages to the OLCAO method. First, the orthogonalization to the core procedure (or the frozen core approximation) reduces the dimension of the final secular equation and speeds up the self-consistent iterations, making it applicable to complex biomolecular systems of up to thousands of atoms. Second, the atomic description of the basis function allows us to use the Mulliken scheme²⁹ to resolve the total density of states (DOS) into atom- and orbital-resolved (or even spin-resolved) partial components, or partial DOS (PDOS). The PDOS is a concept widely used in solid-state physics, and provides information on the number of energy states per unit range of energy and the parentage of the state. The PDOS for each individual atom or a group of atoms in a complex molecule is particularly useful because it can pinpoint the complicated interatomic and intermolecular interactions of specific functional groups in a graphic form. The PDOS result can be compared with experimental data from resonant X-ray photoemission spectra, which explore the valence band states of the molecule, as was demonstrated in refs 23 and 24. Third, the Mulliken scheme can also provide effective atomic charge Q_{α}^* on atom α , and bond order $\rho_{\alpha,\beta}$ between pairs of atoms (α and β) which are defined as

$$Q_{\alpha}^* = \sum_i \sum_{n,occ} \sum_{j,\beta} C_{i\alpha}^n C_{j\beta}^n S_{i\alpha,j\beta} \quad (1)$$

$$\rho_{\alpha,\beta} = \sum_i \sum_j C_{i\alpha}^n C_{j\beta}^n S_{i\alpha,j\beta} \quad (2)$$

In eqs 1 and 2, $C_{i\alpha}^n$ is the eigenvector coefficients of the n th state; $S_{i\alpha,j\beta}$ is the overlap integral between wave functions with atomic specifications of α and β and orbital specifications of i and j . Q^* is the total number of electrons on the α atom. The effective charges provide information on atomic charge transfer, and the bond order is a quantitative measure of the strength of the bond between a pair of atoms. Since Mulliken analysis is more accurate when the basis functions are localized, it is customary to calculate Q_{α}^* and $\rho_{\alpha,\beta}$ using a separate minimal basis set calculation. The net charge on atoms are calculated by subtracting Q^* from the number of their valence electrons.

On the basis of the accurately determined crystal structures, the electronic structure of AdoCbl molecule was calculated using the OLCAO method. In contrast to previous theoretical investigations on Co (corrin),^{14,15} the present calculation includes all the atoms in the side chain of the molecule. An extended basis set consisting of atomic orbitals of Co (1s,2s,2p,3s,3p,4s,4p,3d, 5s,5p,4d), C, N, and O (1s,2s,2p,3s,3p), P (1s,2s,2p,3s,3p,4s,4p,3d), and H (1s,2s,2p) was adopted. Then, the secular equation has a dimension of 1387. More than 60 iterations are needed to have a fully converged self-consistent potential when the eigenvalues stabilize to within 0.00001 eV.

Results

X-ray Structure. X-ray analysis showed that the acetone content per Co atom is 1.25 as compared with that of 0.15

(25) (a) Otwinowski, Z.; Minor, W. *Methods Enzymol.* **1996**, *276*, 307. (b) Sheldrick, G. M. *SHELXL-97*; Universität Göttingen: Göttingen, 1997.

(26) Ching, W. Y. *J. Am. Ceram. Soc.* **1990**, *73*, 3135–60. Ching, W. Y. In *The Magnetism of Amorphous Metals and Alloys*; Fernandez-Baca, J. A., Ching, W. Y., Eds.; World Scientific: Singapore, 1995; pp 85–141.

(27) Hohenberg, P.; W. Kohn, W. *Phys. Rev. B* **1964**, *136*, B864–B871.

(28) Kohn, W.; Sham, L. J. *Phys. Rev.* **1965**, *140*, A1131–1138. Sham, L. J.; Kohn, W. *Phys. Rev.* **1966**, *145*, 561–567.

(29) Mulliken, R. S. Electron Population Analysis on LCAO-MO Molecular Wave Functions. I. *J. Am. Chem. Soc.* **1955**, *23*, 1833–1840. Mulliken, R. S. Electron Population Analysis on LCAO-MO Molecular Wave Functions. II. *J. Am. Chem. Soc.* **1955**, *23*, 1841–1846.

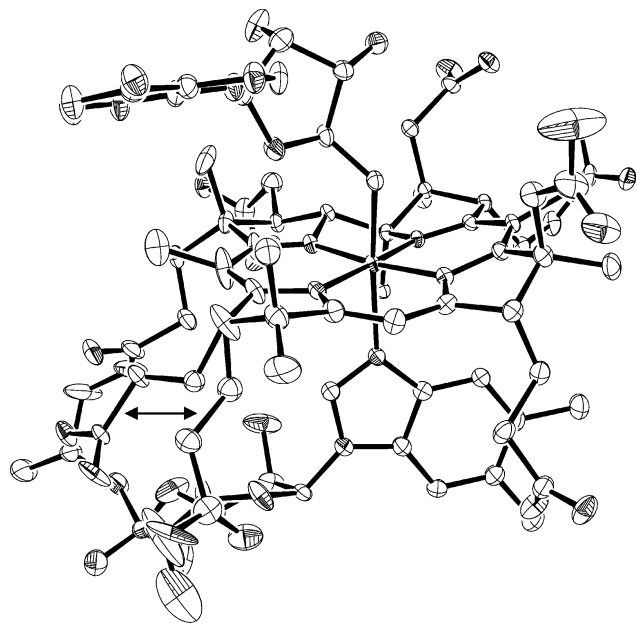


Figure 1. ORTEP drawing of AdoCbl. Atoms are drawn at the 30% probability level. The two orientations of the e chain are both reported and indicated by the double arrow.

detected in the AdoCbl crystal structure, determined by neutron diffraction at 15 K.¹⁶ However, the unit cell parameters are very similar.

An ORTEP drawing of AdoCbl is shown in Figure 1. The superimposition of the non-H atom skeletons of AdoCbl, obtained from neutron and X-ray data, is shown in Figure 2. They superimpose quite well, with only some conformational changes involving the adenosyl and ribosyl moieties and the e amide chain (Scheme 1). In the present structure the latter has two distinct conformations with half-occupancy each. One of the two conformations superimposes well with that found in the neutron structure. This conformational difference should be attributed to the different acetone content. In fact, the acetone molecule with half-occupancy (the other having 0.75 occupancy) is located in the same region where one of the two conformations of chain e is located.

The coordination bond lengths and angles in the present structure do not differ dramatically from those previously reported,^{16,30} as well as the Co–CH₂–C angle (Table 2). However, that the accuracy (as measured by the estimated standard deviations on distances) of the AdoCbl X-ray structure is higher than the neutron one can be appreciated.

The axial distances and some other physicochemical properties of CNCbl, MeCbl, and AdoCbl are compared in Table 2. These data show that there are significant differences in the geometry of the axial fragment, in ground-state physicochemical properties, and in the half-wave potentials, $E_{1/2}$, between the two coenzymes. On the other hand, it has been shown that the Co–N equatorial distances are essentially unaffected by the change in the axial R ligand.³⁰

(30) The two short Co–N21 and Co–N24 distances^{21,22} average to 1.876 (4) Å in both coenzymes, and the two long Co–N22 and Co–N23 ones average to 1.920 (4) and 1.915 (3) Å in MeCbl and AdoCbl, respectively.

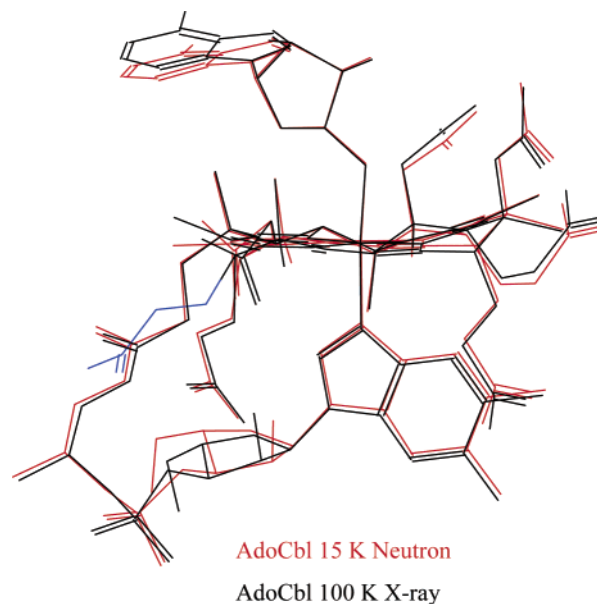


Figure 2. Superimposition of AdoCbl skeletons from neutron (red) and X-ray (black) data. One of the two orientations of the e chain is in blue.

Comparison of data in Table 2 shows the following:

(i) There is a significant lengthening of the Co–N bond in AdoCbl, indicating that Ado exerts a trans influence greater than that of Me.

(ii) The Co–C bond is appreciably lengthened in AdoCbl. Correspondingly, the $\nu_{\text{Co-C}}$ frequency and the Co–C bond dissociation energy (BDE) decrease. Therefore, the Co–C bond in AdoCbl should be weaker than that in MeCbl. The weakening appears to be related to the larger bulk of the Ado group, which is only partially released by the unusual opening of the Co–C(sp³)–C angle up to 123°. However, a contribution to this lengthening (weakening), due to the different electronic properties of Ado and Me, cannot be ruled out, as suggested in simple models.³¹

(iii) The lengthening of the axial distances in AdoCbl with respect to MeCbl corresponds to a less negative value of $E_{1/2}$, i.e., to a less electron rich cobalt center.

The above experimental evidence supports the notion that the Co–C bond in MeCbl is stronger than that in AdoCbl. However, it does not find correspondence in the results of theoretical calculations described below.

Theoretical Calculations. Recent DFT theoretical calculations on corrins focused on factors which could enhance the Co–C homolysis. Optimization of the geometry of R–Co–corrin–base (with several R and L axial base ligands), confirmed¹⁴ spectroscopic data^{6,7} that variation of L has little effect on the Co–C bond. Calculations indicate that Ado(corrin)L has ca. 5 kcal/mol higher HOMO and LUMO energy with respect to the methyl analogue, when L = 5,6-dimethylbenzimidazole (bzm). This finding was claimed to be a theoretical explanation as to why AdoCbl undergoes homolysis more easily and MeCbl undergoes heterolysis more easily.^{14c}

(31) Randaccio, R.; Geremia, S.; Zangrando, E.; Ebert, C. *Inorg. Chem.* **1994**, *33*, 4644–4650.

Table 2. Comparison of Some Geometric Parameters (esd's in Parentheses), and Spectroscopic, Electrochemical and Thermodynamic Properties of the Axial Fragment in MeCbl, AdoCbl, and CNCbl

	Co–C (Å)	Co–NB3 (Å)	Co–C–C (deg)	$\nu_{\text{Co–C}}^a$ (cm ⁻¹)	$E_{1/2}^b$ (V)	BDE ^c
MeCbl	1.979 (4) ^d	2.162 (4) ^d		506	-1.60	37 ± 3
AdoCbl (X-ray)	2.030 (3) ^e	2.237 (3) ^e	123.4 (2) ^e	430	-1.35	30 ± 2
AdoCbl ^f (neutron)	2.023 (10)	2.214 (9)	122.6			
CNCbl ^d	1.886 (4)	2.041 (3)	180.0 (1)			

^a Reference 6; data were obtained with resonance Raman spectroscopy. A similar value of 500 cm⁻¹ for crystalline MeCbl was obtained by Fourier transform Raman spectroscopy (Nie, S.; Marzilli, P. A.; Marzilli, L. G.; Yu, N. T. *J. Chem. Soc., Chem. Commun.* **1990**, 770–771). ^b Lexa, D.; Saveant, J. M. *J. Am. Chem. Soc.* **1978**, *100*, 3220–3222. Sheperd, R. E.; Zhang, S.; Dowd, P.; Hoi, G.; Wick, B.; Choi, S. *Inorg. Chim. Acta* **1990**, *174*, 249–256. ^c Martin, B. M.; Finke, R. G. *J. Am. Chem. Soc.* **1992**, *114*, 585–592. BDE = Co–C bond dissociation energy toward homolysis in kcal/mol. ^d Reference 22. ^e Present work. ^f Reference 18.

Table 3. Net Charge (NC) on Co and Donor Atoms and BO of Coordination Bonds^a

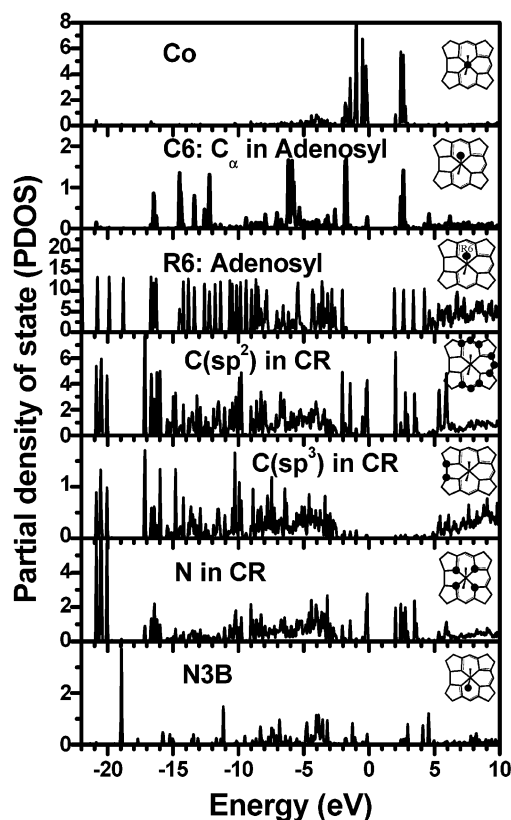
	CNCbl ^b	MeCbl ^c	AdoCbl
NC(Co)	+0.72	+0.71	+0.71
NC(NB3)	-0.35	-0.34	-0.36
NC(C)	+0.01	-0.81	-0.58
NC(N21–24) ^d	-0.30	-0.32	-0.31
NC(N22–23) ^d	-0.36	-0.36	-0.36
BO(Co–C)	0.25	0.13	0.15
BO(Co–NB3)	0.18	0.16	0.15
BO(Co–Neq) ^d	0.21	0.23	0.23

^a NC is derived by subtracting Q^* from the number of valence electrons of the given atom. ^b Reference 23. ^c Reference 24. ^d Mean values.

However, in all the above calculations wave functions of the electronic state were not explicitly discussed. Wave function and charge distribution are important aspects of the electronic structure. In Table 3, we list the calculated Mulliken charges and bond orders in the AdoCbl molecule and compare them with the results of similar calculations on MeCbl²⁴ and CNCbl.²³ Only those atoms bonded to Co are listed.

For the net charges, we observe that (1) Co as a cation loses about 0.7 electron. (2) The net charges on the N atoms in the corrin ring (N21, N22, N23, N24) are similar. On average, each N gains about 0.33 electron. (3) The net charge of NB3 is -0.36. (4) The net charge of the C atom bonded to Co, C α , is -0.58. (5) The net charge for the C atoms in the corrin ring ranges from +0.13 to -0.33 (not listed, but very similar to those in refs 23 and 24), indicating a resonant-like character for C in the corrin ring. (4) The net charges of all the other atoms in the molecule are similar to those in CNCbl²³ and MeCbl.²⁴ (5) With the exception of the C atom bond to Co, the corresponding net charges in all three molecules are very close to each other. The situation is slightly different in the case of bond order. We find the bond order for the Co–C in AdoCbl, MeCbl, and CNCbl to be 0.15, 0.13, and 0.25, respectively. Thus, in AdoCbl, the Co–C bond order is only slightly higher than that in MeCbl and much lower than that in CNCbl. On the other hand, the bond order of Co–NB3 is only 0.15, much less than that of 0.23 for the Co–Neq bond. In all three cases, the C–N bonds in the corrin ring are stronger than the C–C bonds, and the Co–NB3 bond is weaker than the Co–N bonds in the ring. Therefore, the corrin ring has a fairly rigid perimeter with weaker bonds in the middle where the metal ion sits.

Figure 3 shows the PDOS in AdoCbl. We focus the PDOS on the following seven groups: (1) Co; (2) C α ; (3) the other atoms of Ado; (4) sp² bonded C atoms in the corrin ring;

**Figure 3.** Calculated PDOS of AdoCbl: Co, C α , the rest of atoms in Ado, C in CR, N in CR, and N3B.

(5) sp³ bonded C atoms in the corrin ring; (6) N atoms in the corrin ring; (7) N3B atom. Similar PDOS on any atom or groups of atoms in the molecule can be obtained. The following facts are observed: (1) There is clearly a gap of about 2.0 eV separating the occupied and unoccupied Co states. The HOMO state involves the orbitals from Co, and N and C atoms in the corrin ring. From the inspection of the wave functions, it is determined that the occupied ones are the t_{2g} (xy, yz, zx) states and the unoccupied ones are the e_g states (x² - y², 3z² - r²). (2) There is very little participation of Co orbitals in the LUMO state. The LUMO state is dominated by the C–N and C–C interactions in the corrin ring and in the Ado group. (3) The PDOS for N3B and those N atoms in the corrin ring are different. The strong peaks near -19 eV are from the N 2s orbitals. This level is at a higher binding energy than the N atoms in the corrin ring. (4) The R6 panel contains all the atoms of Ado, excluding C α (see Scheme 1). Their PDOS are distributed over all energy ranges except in the top 2 eV region near

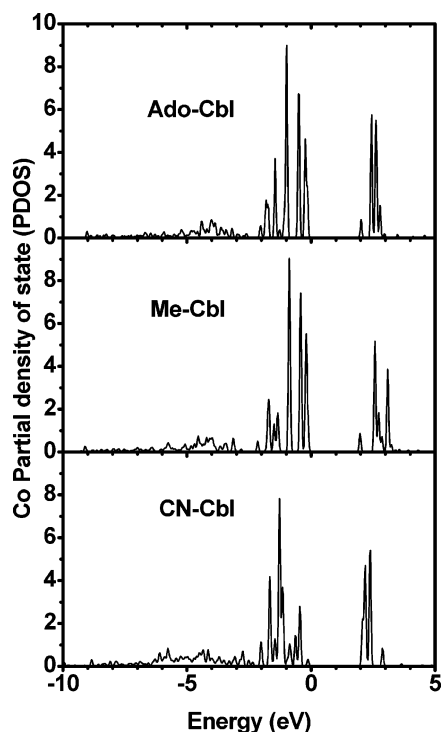


Figure 4. Comparison of PDOS of Co in AdoCbl, MeCbl, and CNCbl. The spectra are all slightly broadened.

the HOMO, where they are conspicuously absent. On the other hand, they contribute significantly to the LUMO state. The strong peaks below -18 eV in the Ado molecule come from the localized states of strong C–O and C–N bonds in the molecule. (5) In the C6, i.e., C α , panel for AdoCbl, the strong bonding peaks with the H atoms in MeCbl²⁴ are no longer present, but the Co–C bonding and the antibonding states are similar. The Co–C antibonding state in AdoCbl is at a slightly lower energy level (2.5 eV), indicating the influence of other atoms on the Co–C bond in the two molecules.

In Figure 4, we compare the PDOS of Co in AdoCbl, MeCbl, and CNCbl. It can be seen that the local PDOS for Co in AdoCbl and MeCbl are only slightly different, mainly in the unoccupied states. However, they differ quite significantly from the PDOS of Co of CNCbl. In the latter case, the HOMO state has negligible Co component. On the other hand, the LUMO state in CNCbl is significantly enhanced with Co 3d orbitals. This is consistent with the fact that the net charge on the C in CN of CNCbl is $+0.01$ compared to those for C of -0.81 and -0.58 for MeCbl and AdoCbl, respectively. It is also consistent with the much larger bond order for Co–C in the case of CNCbl.

Discussion

Comparison of the net charges for CNCbl,²² MeCbl,²³ and AdoCbl shows that they are essentially equal for all the corresponding atoms, with the exception of the C α atom (Table 3). The net charge of the latter is $+0.01$, -0.81 , and -0.58 for CNCbl, MeCbl, and AdoCbl, respectively. This result seems to reflect principally the electronic influence of the different substituents on C α (Scheme 1). However,

the nature of R does not appear to affect the net charge of the metal center or the other five N donors. This does not agree with the previous conclusions,^{14a,c} based on DFT geometry optimization of the analogous corrins, that the Ado group induced more electronic charge density on Co than Me. The net charges on the N21, N24 donor pair are slightly less negative than those on the N22, N23 donor pair, and correspondingly the Co–N21 and Co–N24 distances are shorter than the Co–N22 and Co–N23 ones.³⁰ The bond orders (BOs) are very similar for all the bonds in the three cobalamins, if the Co–C bond and a slight decrease in the Co–NB3 bond order from CNCbl to AdoCbl are excluded (Table 3). These results are consistent with the structural data^{21,22} which suggest that the change in R affects significantly only the axial distances. Furthermore, the trend in BOs within the delocalized moiety of the corrin ring (equal in the three cobalamins) reflects that of the experimental distances.^{21,22} The Co–CN BO is about twice those of the Co–Me and Co–Ado bonds, suggesting a significant Co to CN π back electron donation, i.e., a significant Co–CN double bond character. *Unexpectedly, the Co–C bond order in AdoCbl is essentially equal to or even higher than that in MeCbl.* This could contrast with experimental data, reported in Table 2 (bond lengths, BDEs, and stretching constants), which suggest that the Co–Me bond is significantly stronger than the Co–Ado bond.

It may be appropriate to compare our ab initio calculation using the OLCAO-LDA method to the recent calculation of Jensen et al.,^{14c} who have performed the DFT calculations on B₁₂ models that contain the entire corrin ring. However, all the side chains including the important nucleotide loop which contains the strongly electron negative PO₄ group were neglected. Although both calculations are based on DFT, there are significant variations in the approach, computational algorithm, exchange-correlation functional, and, most importantly, the aim of the calculation. Jensen et al.'s work focused mainly on the geometry optimization of the corrin ring with different models of the attached α -axial ligands. They used the B3LYP potential and hybrid basis functions. The accuracy of the relative energies is the most important issue in determining various bond lengths and bond angles. They showed that the HOMO–LUMO gaps of the eight models studied differ very little, in the 3.3–3.4 eV range. Unfortunately, the calculated Co–NB3 (N_{ax}) bond distance in MeCbl differs from the measured value by 0.14 Å, or 6.4%, indicating a possible deficiency in the calculation. They also found large differences in the equilibrium structure of the CNCbl model from those of MeCbl and AdoCbl. It should be noted that Jensen and Ryde have suggested that the B3LYP DF approach seems to be a problem in calculating the BDE energies in MeCbl.^{14d} This large difference could reflect the small energy differences with respect to the conformational changes in these molecules.

Andruniow, Kozłowski, and Zgierski^{14f} also used a similar method to perform time-dependent DFT calculations on some of the truncated B₁₂ models. The significance of their work is the calculation of an absorption spectrum for vitamin B₁₂,

which showed good agreement with the measured data, if a shift in the energy scale is applied.

In contrast, the present study aims at the electronic structure and bonding in B₁₂ coenzymes using the highly accurate experimentally determined molecular structure. Thus, the full molecule is used, with all the side chains included in the calculation to avoid the need for geometry optimization. Using atomic basis functions and an effective orthogonalization to the core scheme, a fully self-consistent quantum mechanical calculation of this large and complex molecule was accomplished. The results enable us to understand the energy spectrum in terms of atom-resolved PDOS and the effects of charge transfer and bond strength using the effective charge and bond order calculations. Our calculated HOMO–LUMO gaps for the three cobalamins CNCbl, MeCbl, and AdoCbl are 1.96, 2.09, and 2.00 eV, respectively. They are smaller than those of ref 14c (3.38, 3.33, and 3.31 eV in the same order). This can be attributed mainly to the differences in the computational methods and to the different molecular geometries used in the respective calculations. Remarkably, both calculations show that the electronic structure of CNCbl should be significantly different from those of MeCbl and AdoCbl, and that their variations in the HOMO–LUMO gap should be small.

Finally, the efficiency and the versatility of our computational method for complex biomolecular systems have been

fully demonstrated. We expect to extend our investigations to include the presence of solvent molecules and their effects on the overall electronic structure of the B₁₂ molecules.

In conclusion, this analysis suggest that the electronic structure reflects most of the features of cobalamins, as well as the differences between them, and can be considered as a good starting base to examine the modifications induced on the Co–C bond by electronic and steric perturbations. In the case of CNCbl and MeCbl, the calculated electronic structure is in good agreement with the soft-X-ray fluorescence measurements.^{23,24} It is highly desirable that similar measurements can be extended to AdoCbl as well.

Acknowledgment. The work at Trieste is supported by the CofinLab scheme of Ministero dell'Istruzione, Università e Ricerca (MIUR), Rome, Italy. Work at UMKC was supported in part by the U.S. Department of Energy under Grant DE-FG02-84DR45170. Supercomputer time allocation at the National Energy Research Supercomputer Center (NERSC) of DOE is greatly appreciated.

Supporting Information Available: Crystallographic information in CIF format. This material is available free of charge via the Internet at <http://pubs.acs.org>.

IC0348446